

## Using gamma-ray microcalorimeters to lower uncertainty in non-destructive analysis measurements through improvement of nuclear reference data

A. Wessels(2), D.T. Becker(2), D.A. Bennett(2), M. H. Carpenter(3), M. Croce(3), J.W. Fowler(1,2), J. D. Gard(1), J. Imrek(4), K.E. Koehler(5), J.A.B. Mates(2), D.J. Mercer(3), N.J. Ortiz(2), C.D. Reintsema(2), D.R. Schmidt(2), K.A. Schreiber(3), D.S. Swetz(2), J.N. Ullom(1,2), L.R. Vale(2), D.T. Vo(3)

(1) University of Colorado, Boulder, Colorado, USA

(2) National Institute of Standards and Technology, Boulder, Colorado, USA

(3) Los Alamos National Laboratory, Los Alamos, New Mexico, USA

(4) Theiss Research, La Jolla, California, USA

(5) Houghton University, Houghton, New York, USA

### Abstract

Increased accuracy in nuclear non-destructive analysis measurements will improve safeguarding of nuclear facilities. Superconducting microcalorimeters are an emerging technology which achieves better energy resolution than High-Purity Ge (HPGe) detectors at 100 keV by a factor of about ten, which enables them to acquire ultra-high-resolution gamma-ray spectra for isotopic analysis of nuclear materials. Due to their unique combination of collecting efficiency and resolving power, these devices are also capable of performing accurate measurements of fundamental nuclear and x-ray parameters. Detailed analysis of both HPGe and microcalorimeter spectra has shown that improvements in measurements of photon branching ratios, line energies and actinide x-ray linewidths could lead to significant improvements in accuracy of extracted isotopic ratios for both microcalorimeters and HPGe detectors. This is because values for several fundamental parameters are required to determine isotopic ratios from gamma-ray spectra.

Here we will present work being done with microcalorimeters to improve nuclear reference data, and potential future measurements that are feasible with this technology. We will describe past and ongoing measurements of branching ratios, and recent analysis done to extract actinide x-ray linewidth values from the 100 keV region of Pu spectra. Additionally, we will discuss analysis methods and the benefits of using microcalorimeters for this type of analysis.

### Introduction

Gamma-ray transition edge sensor microcalorimeters (TESs) are a powerful emerging technology for non-destructive analysis (NDA) of nuclear materials. These devices are used for ultra-high-resolution gamma-ray spectroscopy for isotopic analysis of nuclear materials. Their (~10x) increased resolving power compared to widespread HPGe technology has spurred investigations into the uncertainty limits of NDA, as these devices have the potential to make more accurate measurements of isotopic ratios. In 2014, Hoover et al. [5] published a study detailing the uncertainty limits in Pu isotopic analysis for both HPGe and microcalorimeter gamma-ray spectra. They found that uncertainties in isotopic mass ratios derived from microcalorimeter data were much less sensitive to uncertainties in nuclear reference data. The accuracy of both microcalorimeter and HPGe gamma-ray spectroscopy is limited by uncertainties in photon branching ratio values. Gamma-ray peak energy uncertainty also contributes significantly to uncertainties in isotopic ratios measured using HPGe. Another

contributor is the uncertainty in the natural linewidths of the actinide K alpha x-ray which are present in the emission-line-dense 100 keV region of Pu spectra. These x-ray peaks are relatively broad and overlap with several gamma-ray lines, as shown in Figure 1.

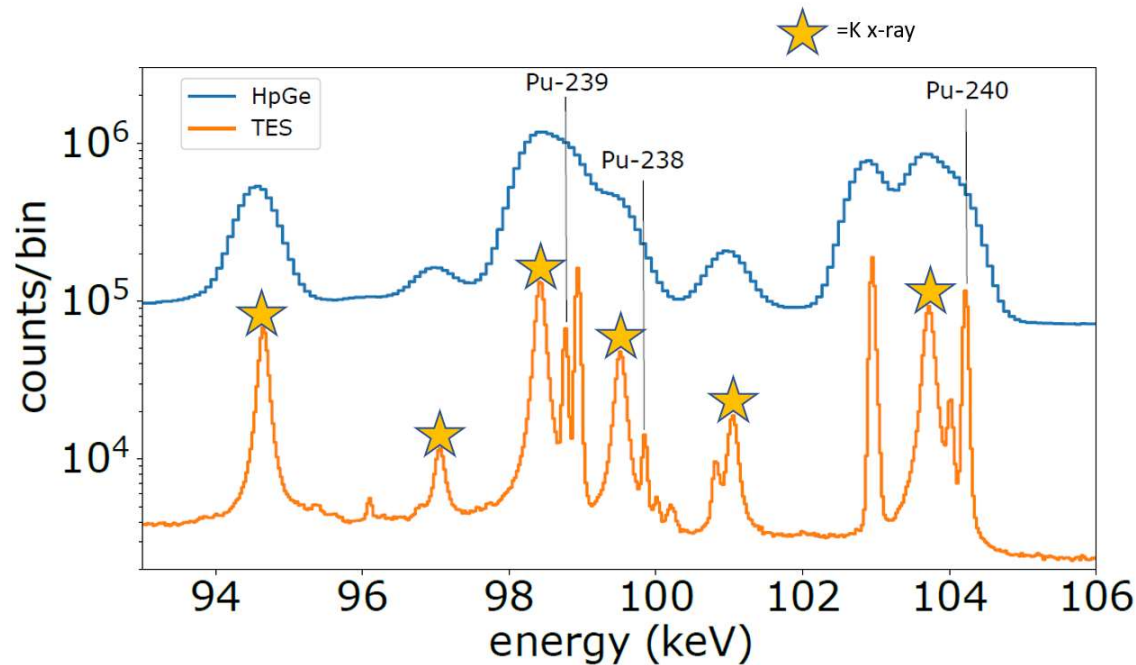


Figure 1: Comparing a CBNM93 spectrum taken with a TES microcalorimeter spectrometer to a HPGe spectrum. The stars indicate K alpha x-ray emission lines of Pu, U and Np. Three Pu gamma-rays which are close to x-ray lines are labelled.

The energy resolution of gamma-ray microcalorimeters can be leveraged for improved measurement of fundamental parameters, and lower uncertainty measurements directly benefit NDA that is carried out with more common HPGe technology. Work is underway to improve fundamental parameter measurements using spectra taken with microcalorimeters. In 2020 Yoho et al. [10] were able to substantially lower uncertainty in branching ratio data for 11 lines of Pu and Am using TES microcalorimeter data and Pu-bearing samples that had been well characterized using mass-spectrometry. New measurements of the peak energy of a Pu-242 gamma-ray near 103 keV have been made with microcalorimeters [7,8]. Improvements in peak locations of other gamma-rays near 100 keV are possible as well, as the x-ray line locations have measurement uncertainties of a few eV and can be used as calibration anchor points to determine the peak locations of nearby gamma-ray peaks, whose peak energy uncertainties are as high as +/-30 eV.

In this paper we will show the advantages of using TES microcalorimeters to analyze the 100 keV region of interest (ROI) of Pu spectrum and extract nuclear reference data, specifically focusing on the  $K\alpha_1$  and  $K\alpha_2$  x-ray linewidths of U, Pu and Np. The analysis of this data is described in detail in Abigail Wessels's dissertation [9]. We will also show the discrepancies between our model of the ROI and the data, and how we are working to reduce model discrepancy.

### Transition edge sensor data acquisition

The data shown here was acquired in March 2021 with the SOFIA (Spectrometer Optimized for Facility Integrated Applications) spectrometer [3] by collaborators at Los Alamos National Laboratory (LANL). The spectrometer routinely achieves a FWHM energy resolution of 75 eV at 100 keV. Data was acquired with 128 multiplexed channels from this instrument. The Pu-bearing samples being measured were nuclear reference material from the Central Bureau for Nuclear Measurements (CBNM) in France. Table 1 shows the composition of the four CBNM samples used.

The datasets contained total photon counts per pixel on the order of  $1e6$  photons. Each dataset was taken within a 40-hour measurement window. To control the count rate of gamma-rays on the detectors and avoid pulse pileup, cadmium shielding material was used between the cryostat and the source. This shielding was 1 mm thick while measuring CBNM93 samples, 1.4 mm thick for CBNM84 samples, and 1.8 mm thick for CBNM70 and CBNM61 samples.

ID	Pu-238	Pu-239	Pu-240	Pu-241	Pu-242	Am-241
CBNM93	0.0093	93.5846	6.3108	0.0557	0.0396	0.2640
CBNM84	0.0565	85.0327	14.2923	0.2577	0.3608	0.9669
CBNM70	0.7046	76.6254	19.0772	1.4203	2.1726	5.3441
CBNM61	1.0075	66.0343	26.7722	1.7547	4.4312	6.6167

Table 1: Composition of the samples, dated April 14, 2015. Isotopic values are in weight percent.

### Extracting actinide x-ray linewidths from CBNM data

The raw microcalorimeter data was processed as described in [2]. Spectra from individual pixels were processed and calibrated before being coadded into a single spectrum. In the 90 to 110 keV region, each x-ray line of interest was used as a calibration point, so that the peaks are well aligned when they are coadded into a single spectrum. Any channels that produced spectra which were not ideal or had energy resolutions above 100 eV were discarded, leaving between 25 and 50 channels which were useable for this analysis.

The full width at half maximum (FWHM) energy resolution of the SOFIA spectrometer is around 75 eV, much wider than the intrinsic linewidths of gamma-rays, so gamma-rays in a microcalorimeter spectra have the line shape of the Gaussian detector response function.  $K\alpha$  x-rays are emitted when an electron from the 2P shell decays into a 1S shell electron hole, meaning their line shape is governed by fundamentally different physics than the nuclear processes which cause gamma-ray emission. Pu, U and Np K alpha x-ray line shapes are Lorentzian, and their natural linewidths ( $\Gamma$ ) are over 100 eV wide. X-rays in microcalorimeter spectra are observed as the convolution of the Gaussian detector response with the Lorentzian function, which is called a Voigt function.

To obtain a high signal-to-noise spectrum, we coadd the spectra from many individual pixels. Each pixel has a Gaussian detector response, but each has a slightly different energy resolution, which means that the detector response of the final coadded spectrum is not Gaussian. We account for this by modeling the coadded detector response as a sum of two Gaussians, one primary Gaussian, and one smaller-amplitude wider Gaussian with the same peak energy which fits the ‘tails’ of the primary Gaussian. The resulting function used to fit x-ray lines is a Lorentzian convolved with these two Gaussians.

The continuum background function typically used for this spectral fitting is the smoothed step function used in [10]. This function depends on the number of counts in the spectrum above and below each point and approximately describes the background due to small angle Compton scattering. The background at energy  $E$  is  $B(E) = B_2 + (B_1 - B_2) \left(1 - \frac{N_{above}(E)}{N_{total}}\right)$ , where  $B_1$  and  $B_2$  are free parameters which determine the background at the lower and upper ends of the spectrum,  $N_{total}$  is the total number of counts in the spectrum and  $N_{above}(E)$  is the number of counts in the spectrum above the energy  $E$ . Spectra from SOFIA contain another component of the background referred to as Sn escape peaks. These peaks are due to Sn x-rays from the TES absorber being emitted after a gamma-ray is absorbed, causing a phantom peak to appear at the gamma-ray energy minus the energy of the outgoing x-ray. Reference [10] reported escape peak yields calculated from Pu spectra taken with a similar microcalorimeter array, and I used these values to fix the amplitudes of the Sn  $K\alpha_1$ ,  $K\alpha_2$  and  $K\beta$  escape lines relative to one another.

As described in [5], one of the challenges facing TES gamma-ray spectroscopy is problems with model discrepancy. For our analysis the reduced  $\chi^2$  values from our fits increase significantly as the user selects wider energy ranges to fit over, and as more counts are added to a spectrum through coadding, as was observed by Hoover et al. [5]. This appears to be caused in part by the shortcomings of the continuum background model in modeling the background over the whole 10 keV ROI. The background function contains only two free parameters which are floated during our fits, so we were able to improve spectral fits by fitting the ROI in three pieces and allowing the background parameters to differ for each sub-ROI. ROI I is 94.165 to 95.165 keV and contains the U  $K\alpha_2$  line (see Figure 2). ROI II is 96.5 to 103.5 keV and contains Np  $K\alpha_2$ , Np  $K\alpha_1$ , Pu  $K\alpha_2$  and U  $K\alpha_1$  x-ray lines. ROI III is 102.5 to 104.7 keV and contains the Pu  $K\alpha_1$  x-ray. ROI I contains only one peak, so we used a simple linear background for this portion of the fit, and the step background was used for ROIs II and III. Table 2 lists the peaks and peak energies used in our model of the spectrum and whether the peak was used as a calibration point.

ID	Energy (keV)	Calibration point
U $K\alpha_2$	94.665	yes
Pu-239	96.118	no
Am-241	96.740	no
Np $K\alpha_2$	97.069	yes
U $K\alpha_1$	98.439	yes
Pu-239	98.780	no
Am-241	98.950	yes
Pu $K\alpha_2$	99.529	yes
Pu-238	99.853	no
Np $K\alpha_1$	101.059	yes
Am-241	102.966	yes
Pu-239	103.032	no
Pu-241	102.966	yes
Pu-241	103.680	no
Pu $K\alpha_1$	103.734	yes
Pu-240	104.234	no

Table 2: List of peaks and peak energies included in our model of the 94 to 106 keV energy range and whether they were used as a calibration point.

To fit the data, we used the maximum likelihood least squares fitting procedure for Poisson distributed data described in [4]. This was executed with the Python package lmfit, which allows the user to build up a composite model of many functions to fit a spectrum. We fit all three ROIs simultaneously. We assumed that the detector response function was constant across the 3 ROIs and floated all the detector response function parameters. All x-ray peak energies in ROI II were allowed to float  $\pm 10$  eV during fitting, and in ROI I and III they were floated  $\pm 20$  eV. All gamma-ray peaks were floated by  $\pm 20$  eV, and Sn escape peaks were floated  $\pm 10$  eV. Peak amplitudes were allowed to float and take on any positive value. The x-ray linewidths were given the initial values from Krause and Oliver [6] and allowed to float by  $\pm 15\%$ . The number of free parameters in the fit was 49.

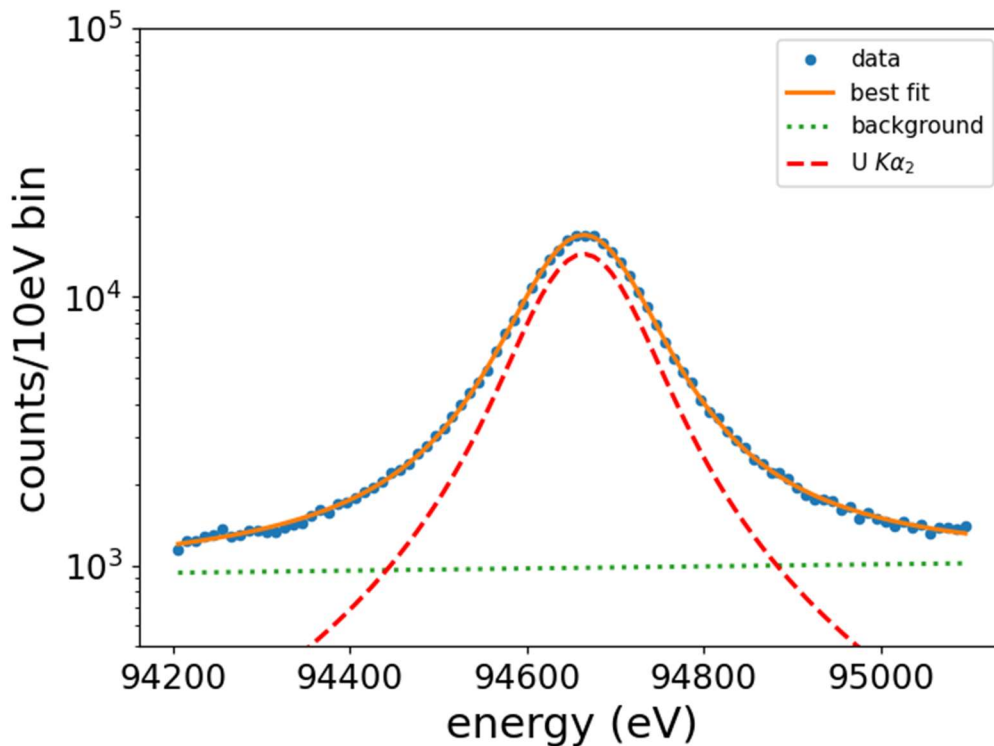


Figure 2: Fit to ROI I of the CBNM93 spectrum. The fitted  $U K\alpha_2$  x-ray line is shown in the dashed red line. The green dotted line is the linear background function.

### Model discrepancy

Model discrepancy is a source of systematic error that can be difficult to quantify. In general, models are imperfect descriptions of the data. This holds true when fitting CBNM spectra, and we found several parts of the spectrum which did not fit the model we had built. One example is shown in Figure 3. This shows the 99.8 to 101.5 keV region of the CBNM93 and CBNM61 spectra. The CBNM93 spectrum has a significant discrepancy between the model and data, while in CBNM61 the data and model match quite well. This suggests that there may be one or multiple peaks missing in our model which are only bright enough to be noticeable in the CBNM93 spectrum.

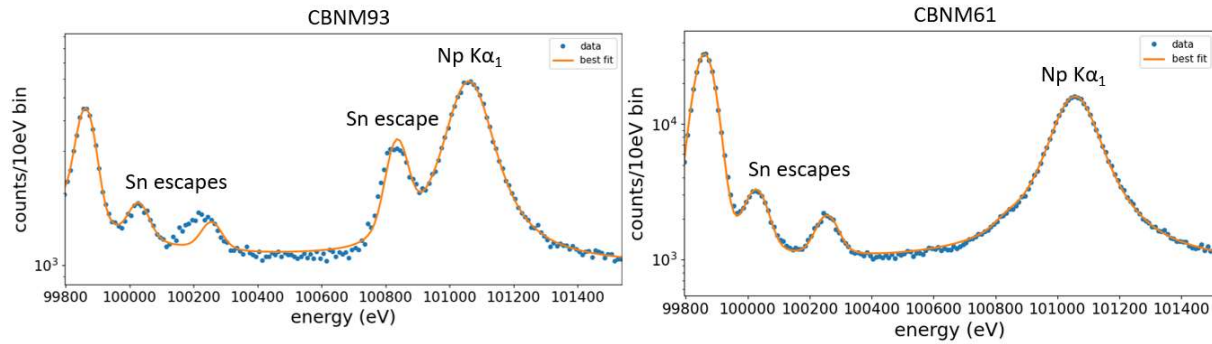


Figure 3: Data and fits in the 99.8 to 101.5 keV range for CBNM93 (left) and CBNM61 (right).

Another place where model discrepancy was observed were the energies adjacent to gamma-ray lines. Since the gamma-ray line shapes in our spectra are identical to the detector response function, this indicates a problem with the assumed detector response function. We typically use a symmetric detector response function which is the sum of two gaussians, as described above. Figure 4 shows this model (black line) being fit to an isolated gamma-ray and the residual from the fit. This figure also shows an asymmetric model where the two gaussians are allowed to have different peak energies, with the smaller Gaussian having a higher peak energy. This model adds one additional free parameter, so we expect this fit to have a better reduced  $\chi^2$  value. In this case the reduced  $\chi^2$  value decreased by about a factor of four, from 8.49 to 1.82. The asymmetric detector response function helps to lower reduced  $\chi^2$  values in fits of the 100 keV region as well. In this example, the Bayesian and Akaike information criteria both dropped by more than a factor of two from the symmetric to the asymmetric model. We do not have a physical explanation for why this detector response function would be asymmetric, and historically we have used a symmetric detector response function, but adoption of the asymmetric model may help to decrease bias in results for both isotopic analysis fits and measurements of nuclear reference data.

As discussed above, we also found that the background model being used was insufficient for fitting a region over 10 keV wide. Figure 5 shows an example fit of CBNM61 data and the background function, which clearly doesn't fit the edges of the ROI properly. Several of the resulting linewidth fits differ in a statistically significant way from both published values and fits that are done with three separate ROIs, and uncertainties in linewidths are up to a factor of 10 higher. A deeper look at the background model typically used for gamma-ray spectroscopy could lessen model discrepancy significantly.

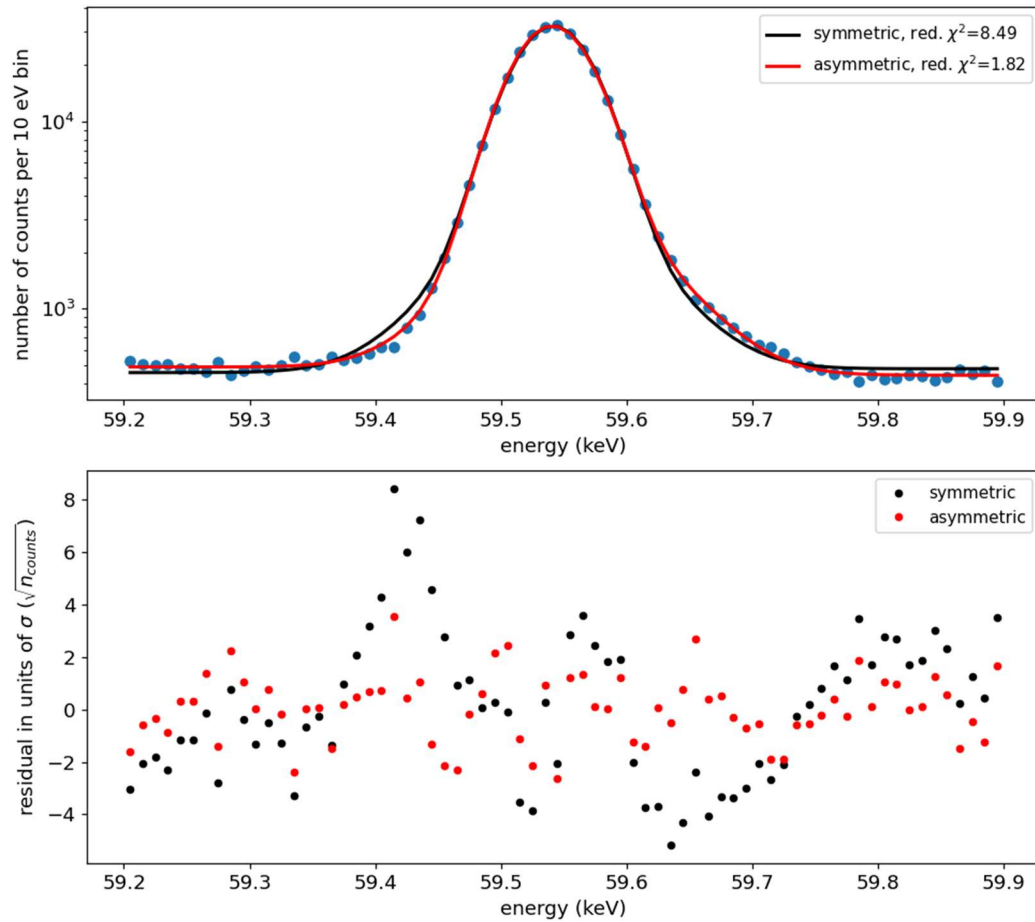


Figure 4: Top: fit of a 60 keV Am-241 gamma-ray peak from a CBNM61 spectrum. The black line represents the symmetric two-gaussian detector response function. The red line is a similar function but the two gaussians are allowed to have different peak energies, making it asymmetric. Bottom: residual of the fits in units of the square root of the number of counts ( $\sigma$ ).

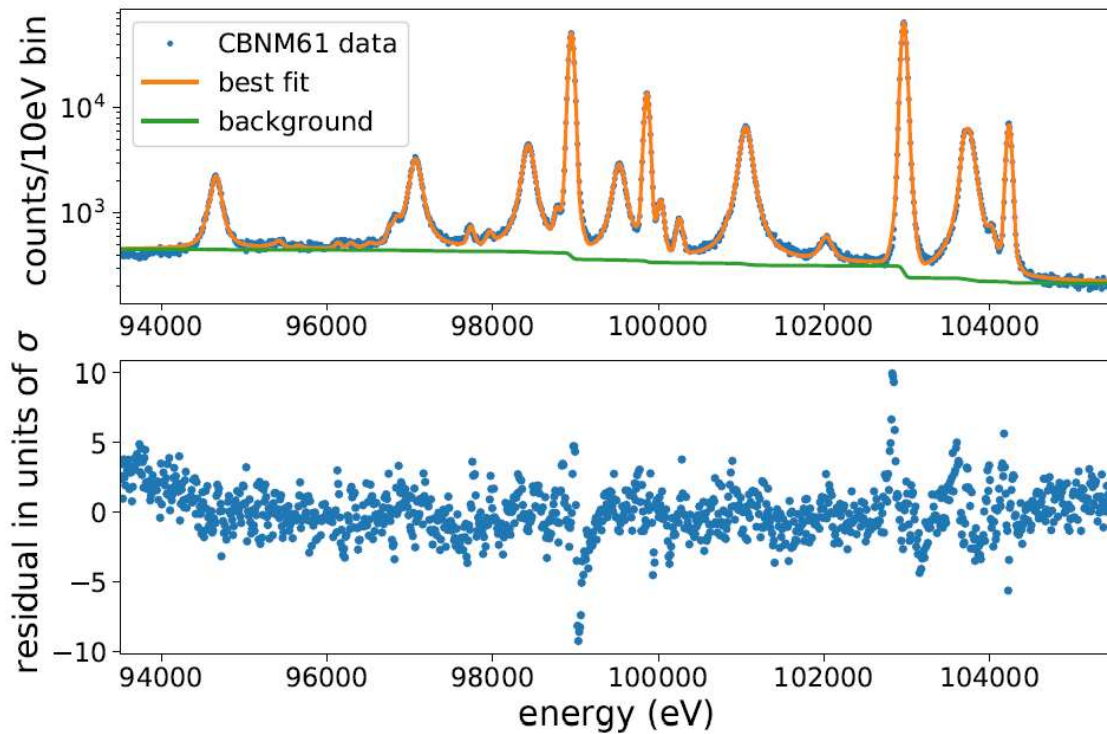


Figure 5: Top: example of a fit to the 93.5 to 105 keV energy range of a CBNM61 spectrum with a step background function. Bottom: residual of the fit, in units of the square root of the number of counts per bin ( $\sigma$ ). This spectrum was fit assuming the symmetric detector response function.

### Future work

TES microcalorimeters offer the resolution at 100 keV needed to improve measurements of fundamental parameters that are needed for isotopic analysis. We intend to fit spectra from each of the CBNM samples and combine the fitted linewidths to achieve a single value for each line. We will then carry out a careful uncertainty analysis to ensure that we report an accurate uncertainty for each linewidth value.

As discussed above, there is work to be done in improving the detector response model, the peak model of the ROI, and the background model. The excellent resolution of TES microcalorimeters allows us to clearly identify shortcomings like missing peaks which would be obscured by a detector with poorer resolution. It may be possible to make the detector response behave more ideally through improvements in TES microcalorimeter design which are currently being explored.

### References

- [1] Barreau, G., et al. "Precision measurements of x-ray energies, natural widths and intensities in the actinide region." *Zeitschrift für Physik A Atoms and Nuclei* 308.3 (1982): 209-213.
- [2] Becker, Daniel T., et al. "Advances in analysis of microcalorimeter gamma-ray spectra." *IEEE Transactions on Nuclear Science* 66.12 (2019): 2355-2363.



- [3] Croce, Mark, et al. "Electrochemical Safeguards Measurement Technology Development at LANL." *Journal of Nuclear Materials Management* 49.1 (2021): 116-135.
- [4] Fowler, Joseph W. "Maximum-likelihood fits to histograms for improved parameter estimation." *Journal of Low Temperature Physics* 176.3-4 (2014): 414-420.
- [5] Hoover, Andrew S., et al. "Uncertainty of plutonium isotopic measurements with microcalorimeter and high-purity germanium detectors." *IEEE Transactions on Nuclear Science* 61.4 (2014): 2365-2372.
- [6] Krause, Manfred O., and J. H. Oliver. "Natural widths of atomic K and L levels,  $K\alpha$  X-ray lines and several KLL Auger lines." *Journal of Physical and Chemical Reference Data* 8.2 (1979): 329-338.
- [7] Mercer, David J., et al. "Quantification of  $^{242}\text{Pu}$  with a Microcalorimeter Gamma Spectrometer." *arXiv preprint arXiv:2202.02933* (2022).
- [8] Teti, Emily et al., "Quantification of  $^{242}\text{Pu}$  with a Microcalorimeter Gamma Spectrometer" these proceedings (2023)
- [9] Wessels, Abigail. *Advances in Superconducting Gamma-Ray Microcalorimeters to Improve Non-Destructive Analysis of Nuclear Materials*. Diss. University of Colorado at Boulder, 2022.
- [10] Yoho, Michael Duncan, et al. "Improved plutonium and americium photon branching ratios from microcalorimeter gamma spectroscopy." *Nuclear Instruments and Methods in Physics Research Section A: Accelerators, Spectrometers, Detectors and Associated Equipment* 977 (2020): 164307.